Soft turbulence in multimode lasers

D. Casini,[1] G. D'Alessandro,[2] and A. Politi[1,3]
[1]*Istituto Nazionale di Ottica, Largo E. Fermi 6, I-50125 Firenze, Italy*
[2]*Department of Mathematics, University of Southampton, Southampton SO17 1BJ, England, United Kingdom*
[3]*Istituto Nazionale di Fisica Nucleare, Sezione di Firenze, Firenze, Italy*
(Received 8 July 1996)

Using a weakly nonlinear analysis, we study the behavior of a homogeneously broadened laser in the vicinity of the second threshold. We show that the dynamics is described by a complex Ginzburg-Landau equation coupled to a Fokker-Plank equation. Although the cubic term of the Ginzburg-Landau equation is destabilizing for all parameter values, bounded solutions exist because of the strong nonlinear dispersion (''dispersive chaos''). A careful numerical study of the original Maxwell-Bloch equations is also carried out to investigate the role played by off-resonant solutions. [S1050-2947(97)02001-5]

PACS number(s): 42.60.Mi, 42.65.Sf, 42.55.−f, 42.65.−k

I. INTRODUCTION

Maxwell-Bloch equations represent the core of many laser models. They are widely employed to describe all types of single-mode laser instabilities [1–3] as well as multimode dynamics. Here, we focus our attention on the behavior of a homogeneously broadened unidirectional laser in the absence of transverse effects. The first two assumptions are dictated, as usual, by the need to make the analytical and numerical investigations as simple as possible, while leaving the qualitative behavior unchanged. The reason for the last restriction represents the main motivation for our paper: to isolate longitudinal instabilities in order to capture the essence of their features.

It has been known for a long time that such a model shows two thresholds as the pump parameter is increased from zero. The first threshold corresponds to the switching on of the laser. Below threshold, no laser field is emitted, while above there is an electric field in the cavity that can be described as a single longitudinal mode solution of the model's equations. As the pump parameter is increased further and further, the single mode solution becomes unstable against perturbations with wave vectors lying in two sidebands [1,2] centered around two opposite wave vectors. Accordingly, the intensity of the laser light starts oscillating and, if the cavity is sufficiently long, an irregular spatial dependence of the field sets in as well.

In small cavities, only one cavity mode can be excited, so that Maxwell-Bloch equations reduce to a set of three ordinary differential equations that have been shown to be equivalent to the Lorenz model. In such a case, the onset of irregular behavior arises only in the bad cavity limit and is, in any case, limited to the time domain while the spatial profile is that of the corresponding cavity mode.

More interesting and experimentally accessible is the case of long cavities, when two new modes are excited. This scenario is very similar to the turbulent flow of a fluid in a pipe: not only the laser output, but also the field spatial dependence along the cavity axis, is irregular. For this reason, this kind of laser behavior has been called Maxwell-Bloch turbulence in Ref. [4], where it has been analyzed in an information theoretical way. Using mutual information, the authors pinpoint the role played by the unstable Rabi side bands: they are the source of the chaotic dynamics and information (energy) flows from them.

The study of Maxwell-Bloch turbulence done in Ref. [4] shows how rich the laser dynamics is and how comprehension of its behavior creates a tool to better understand turbulence in various branches of physics. With this idea in mind we have analyzed in detail the near-threshold laser dynamics: being near the onset of turbulence allows us to use weakly nonlinear analysis to model the laser and thus obtain a partially analytical grip on this complex problem.

The aim of the present paper is to set up a framework for such analysis and develop and test an accurate and reliable model of the near-threshold dynamics of a homogeneously broadened unidirectional ring laser. We show that it can be described by a complex Ginzburg-Landau equation coupled to a Fokker-Planck equation. Moreover, the values of the parameters that control these equations are somewhat peculiar: the Ginzburg-Landau equation has a positive cubic term. Nevertheless, the solutions do not explode because the equation is highly dispersive, a situation that has been analyzed in Ref. [5]. Thus the laser is an optical example of a type of turbulence already found in hydrodynamics [6] and called dispersive chaos: ''a dynamical state in which repetitive pulsing caused by strong nonlinear dispersion produces continuously erratic spatiotemporal behavior'' (quoted from the abstract of Ref. [6]).

The paper is organized as follows: in the next section we introduce the Maxwell-Bloch model of the ring laser and summarize the known properties of the linear stability analysis of the single mode solution. This is important in order to define the proper environment for the perturbation expansion near the second threshold, developed in Sec. III. There, we derive the governing equation for the laser field near the bifurcation point (*amplitude equations*). The dynamical properties of such equations are investigated in Sec. IV. In Sec. V, we discuss the correctness of this approximation by comparing its predictions with those of numerical integration of the model equations and we discuss their validity. Finally, in the conclusions we summarize our results and discuss some possible ways forward.

II. MODEL AND LINEAR STABILITY ANALYSIS

Besides considering the restrictions already mentioned in the Introduction, we further assume that the laser dynamics is well described by mean-field equations; i.e., we postulate that the profile of the field intensity does not exhibit any systematic growth (decay) along the cavity. This approximation becomes increasingly accurate as the reflectance of the cavity mirrors is increased. Anyhow, the spatial dependence has been fully taken into account in Ref. [7] where, however, no relevant difference has been found with the simplified model.

A further remark concerns the detuning Δ between the cavity and the atomic frequency ω_a. We assume it to be zero (resonant case). In short cavities, Δ plays a crucial role, as it heavily affects the first laser threshold. In moderately long cavities, it still plays some role in controlling the switch among the various modes or their simultaneous functioning [8]. In long cavities, Δ loses all meaning: there is always a cavity mode resonant with the atomic frequency and Δ can be always scaled out by changing reference frame.

The laser equations in a frame rotating at frequency ω_a are

$$\partial_t F = \kappa(P - F) + \partial_z F,$$

$$\partial_t P = -P + FD,$$

$$\partial_t D = \gamma_\parallel[-D + \chi - \tfrac{1}{2}(F^*P + FP^*)], \tag{1}$$

where time is normalized to the inverse of polarization decay rate $\gamma_\perp$, while space is normalized in such a way that the speed of light is equal to 1; $\gamma_\parallel$ and κ represent the damping constants of population inversion and electric field, respectively (both again scaled with respect to $\gamma_\perp$). Finally, χ is the pump parameter.

These equations admit single-mode solutions for every possible value of the wave number k, provided that the pump value is above the corresponding threshold,

$$F_0^{(k)} = \sqrt{\chi - (1+\omega_k^2)}\, e^{i\varphi_0^{(k)}} e^{i(\omega_k t + kz)}, \quad P_0^{(k)} = F_0^{(k)}(1 - i\omega_k),$$

$$D_0 = 1 + \omega_k^2, \quad \omega_k = \frac{k}{1+\kappa},$$

where the phase $\varphi_0^{(k)}$ is an arbitrary real number. In fact, there are infinite stationary solutions with the same wave number, one for each value of the phase. This has deep consequences on the dynamics. Namely, the single-mode stationary solution is always marginally stable with respect to a perturbation that changes the phase of the field uniformly across the cavity length. In order to highlight this phenomenon and keep better track of it, it is convenient to introduce polar coordinates; the field and the polarization are expressed as modulus and phase,

$$F = f e^{i\varphi}, \quad P = p e^{i\beta} e^{i\varphi}.$$

The laser equations expressed in the new variables are

$$\partial_t f = -\kappa f + \partial_z f + \kappa p \cos\beta, \tag{2}$$

$$\partial_t p = -p + fD \cos\beta,$$

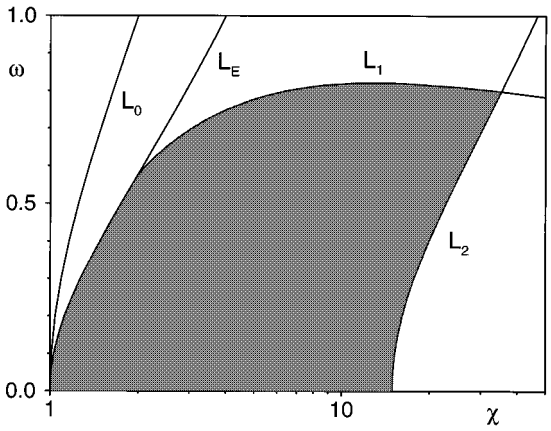

FIG. 1. The shaded region denotes the stability domain of single-mode laser solutions for $\kappa = \gamma_\parallel = 1$. L_0 is the first threshold line, L_E is the line of Eckhaus instability, and L_1 and L_2 are the lines of two distinct Hopf bifurcations.

$$\partial_t D = \gamma_\parallel(-D + \chi - fp\cos\beta),$$

$$\partial_t \beta = -\left(\frac{f^2 D + \kappa p^2}{fp}\right)\sin\beta - \partial_z \varphi,$$

$$\partial_t \varphi = \kappa \frac{p}{f}\sin\beta + \partial_z \varphi.$$

Some preliminary information about the dynamics of the above model is obtained from the linear stability analysis of the single-mode solutions. This can be done by writing the perturbation as the superposition of plane waves with wave number q, an ansatz that reduces the problem to solving a fifth-order algebraic equation for the eigenvalues $\lambda_k(q)$. This means that there exist five branches $\lambda_k^{(i)}(q)$ and the single-mode solution with wave number k is linearly stable if and only if the real part of $\lambda_k^{(i)}(q)$ is negative for all q's and all i's. A particular case is $q=0$ since $\lambda_k(0)=0$ on one of the branches. This reflects the marginal stability against global phase fluctuations, which in turn follows from the arbitrariness of the phase φ.

A general discussion of the stability properties has been carried out in Ref. [9]; here, we first recall the main results and then repeat some of the calculations in the resonant case ($k=0$), as some expressions are needed to derive the amplitude equations in the following section. In Fig. 1, we report the borders of the stability domains with reference to the case $\kappa = \gamma_\parallel = 1$. The line L_0 represents the first laser threshold above which the single-mode solution with wave number k is sustained by the laser cavity ($\chi = 1 + k^2/4$, in the present case) with nonzero amplitude. The line L_E represents the border of the domain of Eckhaus instability: laser modes to the left of L_E are Eckhaus unstable, i.e., the uniform solution is unstable for small but finite q's. Both L_1 and L_2 are marginal stability curves, where a single-mode laser solution becomes unstable under perturbations with (in general) finite wave numbers. More precisely, unstable solutions are placed above L_1 and to the right of L_2. As a result, the shaded region is the only domain where the corresponding single-mode solutions are linearly stable. Notice that above $\chi = 35.2\ldots$, no stable single mode exists. Accordingly, such a

critical value plays a role similar to any point along the Benjamin-Feir line in the parameter space of the complex Ginzburg-Landau equation, although the instability mechanisms are different in the two models.

Numerical simulations performed above L_1 indicate that the instability is practically of Eckhaus type, since it just leads to an adjustment of the wave number k until the stable domain is entered and no chaotic evolution is observed any longer. More interesting is the region to the right of L_2, where, despite the existence of linearly stable solutions, an irregular dynamics is observed. For this reason, we have decided to study perturbatively the resonant single-mode solution, the first to become unstable when increasing χ. Nevertheless, we show in Sec. IV that our approach is also able to account for the effect of small off-resonance effects.

The single-mode resonant stationary solution is $f_0=p_0=\sqrt{\chi-1}$, $\beta_0=0$, and $\varphi=\varphi_0$, an arbitrary constant (from now on, we drop the dependence on k as we will always refer to $k=0$).

The laser equations (2), linearized around this stationary solution, are described by a block diagonal operator,

$$\frac{\partial}{\partial t}\begin{pmatrix}\delta f\\ \delta p\\ \delta D\\ \delta\beta\\ \delta\varphi\end{pmatrix}=\begin{pmatrix}-\kappa+\partial_z & \kappa & 0 & 0 & 0\\ 1 & -1 & f_0 & 0 & 0\\ -\gamma_\parallel f_0 & -\gamma_\parallel f_0 & -\gamma_\parallel & 0 & 0\\ 0 & 0 & 0 & -(1+\kappa) & -\partial_z\\ 0 & 0 & 0 & \kappa & \partial_z\end{pmatrix}\begin{pmatrix}\delta f\\ \delta p\\ \delta D\\ \delta\beta\\ \delta\varphi\end{pmatrix}. \tag{3}$$

After expanding in plane waves of wave vector q, we obtain two separate eigenvalue problems. The 2×2 submatrix gives rise to the solutions

$$\lambda=\frac{-(1+\kappa)+iq\pm\sqrt{(1+\kappa)^2-q^2+2qi(1-\kappa)}}{2}.$$

Both eigenvalues are independent of the pump value. The eigenvalue with the minus sign has a negative real part for all q values, while the real part of the one with the plus sign is exactly zero for $q=0$, where it reaches its maximum value. The ''eigenvector'' corresponding to this zero ''eigenvalue,'' $\mathbf{w}_1\equiv(0,0,0,0,1)$, is the global phase of the field, in agreement with the previous considerations.

The spectrum of the 3×3 submatrix depends implicitly on the value of the pump parameter through f_0. For sufficiently high intensity, a mode of wave number $q=\tilde{q}$ becomes unstable. Accordingly, the amplitudes of the electric field, polarization, and population inversion acquire a modulation of wave number $\tilde{q}$. This is the so-called second laser threshold [1,2], which we show to be a subcritical Hopf bifurcation for all parameter values. Since this study is important in view of the characterization of the evolution in the vicinity of the bifurcation, we go through the various steps in some detail.

The determinant of the 3×3 submatrix is

$$\lambda^3+(1+\gamma_\parallel+\kappa-i\tilde{q})\lambda^2+[\gamma_\parallel(1+\kappa+f_0^2)-i\tilde{q}(1+\gamma_\parallel)]\lambda+2\gamma_\parallel\kappa f_0^2-i\tilde{q}(1+f_0^2)\gamma_\parallel=0. \tag{4}$$

The threshold can be determined by imposing that the maximum value of the real part of λ (upon varying q) is zero. In other words, we must impose that $\lambda=i\nu$ when $\partial_q\lambda=i\partial_q\nu$ where both ν and $\partial_q\nu$ are real numbers representing the frequency of the oscillations at the Hopf bifurcation and its derivative with respect to the wave number q. In this way we can determine both the critical pump value $\tilde{\chi}$ (or, equivalently, $\tilde{f}^2=\tilde{\chi}-1$) and the critical wave number $\tilde{q}$.

Let us start by solving the real part of Eq. (4) with respect to the wave number,

$$\tilde{q}=\frac{(1+\gamma_\parallel+\kappa)\nu^2-2\gamma_\parallel\kappa\tilde{f}^2}{(1+\gamma_\parallel)\nu}. \tag{5}$$

After substituting Eq. (5) in the imaginary part of Eq. (4), we obtain the further constraint

$$\nu^4-\nu^2(3\tilde{f}^2-\gamma_\parallel)\gamma_\parallel+2\gamma_\parallel^2\tilde{f}^2(1+\tilde{f}^2)=0. \tag{6}$$

We can now compute the derivative of Eq. (4) and solve for $\partial_q\nu$, obtaining

$$\partial_q\nu=\frac{-i(1+\tilde{f}^2)\gamma_\parallel+\nu(1+\gamma_\parallel)+i\nu^2}{3i\nu^2+2(1+\gamma_\parallel+\kappa-i\tilde{q})\nu-[i\gamma_\parallel(1+\tilde{f}^2+\kappa)+\tilde{q}(1+\gamma_\parallel)]}. \tag{7}$$

Upon imposing that $\partial_q\nu$ is a real number, i.e., by multiplying the numerator by the complex conjugate of the denominator and imposing that the result is real, one obtains

$$\nu^3(2\kappa-1-\gamma_\parallel)+\tilde{q}(1+\gamma_\parallel)\nu^2-\nu\gamma_\parallel[(1+\tilde{f}^2)(1+\gamma_\parallel)+\kappa(1-\gamma_\parallel+2\tilde{f}^2)]+(1+\tilde{f}^2)(1+\gamma_\parallel)\tilde{q}\gamma_\parallel=0.$$

We can substitute expression (5) to eliminate the $\widetilde{q}$ dependence in the above equation, to obtain

$$3\nu^4+\gamma_\parallel(\gamma_\parallel-3\widetilde{f}^2)\nu^2-2\gamma_\parallel^2\widetilde{f}^2(1+\widetilde{f}^2)=0. \tag{8}$$

Equations (6) and (8) are very similar to one another. By summing them, we obtain a simple solution for the frequency at threshold $\widetilde{\nu}$,

$$\widetilde{\nu}^2=\tfrac{1}{2}(3\widetilde{f}^2-\gamma_\parallel)\gamma_\parallel. \tag{9}$$

By substituting back in Eq. (6), we find an analytic expression for the pump parameter [9]

$$\widetilde{\chi}=\widetilde{f}^2+1=5+3\gamma_\parallel+2\sqrt{2}\sqrt{2+3\gamma_\parallel+\gamma_\parallel^2}, \tag{10}$$

which is independent of the (rescaled) field decay rate κ. Let us stress that this cancellation of the parameter dependence is not obvious at all: it does not follow from any scaling of the variables. The same comment applies to the frequency $\widetilde{\nu}$ of the bifurcating solution, another quantity that is independent of κ. Notice also that since $\widetilde{\nu}\neq 0$ for all parameter values, the bifurcation is always of Hopf type.

A compact expression for the wave number is obtained by partially substituting Eq. (9) into Eq. (5)

$$\widetilde{q}=\widetilde{\nu}-\kappa\,\frac{\gamma_\parallel(\widetilde{f}^2+\gamma_\parallel)}{2(1+\gamma_\parallel)\widetilde{\nu}}, \tag{11}$$

showing that the wave number does, instead, depend on κ. In particular, we see that $\widetilde{q}$ can be equal to zero. In other words, for special values of $\gamma_\parallel$ and κ this instability can be observed even in short cavities.

III. NONLINEAR ANALYSIS

The linear stability analysis developed in the previous section tells us that the single-mode solution has always a marginally stable mode with wave vector $q=0$, which corresponds to the phase invariance of the single-mode solution. At threshold, a second mode, with wave vector $q=\widetilde{q}$, is marginally stable. Nonlinear analysis builds on this knowledge to obtain the equations, the *amplitude equations*, obeyed by the amplitudes of these two modes in a neighborhood of the bifurcation point [10].

We introduce a vector $\mathbf{u}$ that represents the difference between the values of the fields f, p, D, φ, and β and their stationary values at threshold,

$$\mathbf{u}=\begin{pmatrix} f\\ p\\ D\\ \varphi\\ \beta\end{pmatrix}-\begin{pmatrix}\widetilde{f}\\ \widetilde{p}\\ \widetilde{D}\\ \widetilde{\varphi}\\ \widetilde{\beta}\end{pmatrix}.$$

Call ε a small parameter that measures the distance of the control parameter, the pump intensity, from the bifurcation point: at the bifurcation point $\varepsilon=0$. Near the bifurcation point, we can expand $\mathbf{u}$ in powers of ε,

$$\mathbf{u}=\mathbf{u}_0+\varepsilon\mathbf{u}_1+\varepsilon^2\mathbf{u}_2+O(\varepsilon^3),$$

where

$$\mathbf{u}_0=\varphi_{00}\mathbf{w}_1,$$

$$\mathbf{u}_1=\mathbf{u}_{10}+\frac{1}{2}\,[L_{11}\mathbf{w}_2e^{i(\widetilde{q}z-\widetilde{\omega}t)}+\text{c.c.}],$$

$$\mathbf{u}_2=\mathbf{u}_{20}+[\mathbf{u}_{21}e^{i(\widetilde{q}z-\widetilde{\omega}t)}+\text{c.c.}]+[\mathbf{u}_{22}e^{i(2\widetilde{q}z-2\widetilde{\omega}t)}+\text{c.c.}].$$

The subindices of different variables have always the same meaning: the first index refers to the order in ε, the second to the value of the wave vector, measured in multiples of $\widetilde{q}$. Therefore, φ_{00} is the zero-order amplitude of the mode with wave vector $q=0$, $\mathbf{u}_{10}$ is a vector that represents the terms at first order in ε with wave vector $q=0$, and L_{11} is the amplitude of the marginally stable mode ($q=\widetilde{q}$) at first order in ε. $\mathbf{w}_1$ is the marginally stable eigenvector at $q=0$, while $\mathbf{w}_2$ is the marginally stable eigenvector at $q=\widetilde{q}$. The marginally stable mode $\mathbf{w}_1$ appears already at order zero because the stationary solution is marginally stable with respect to this mode independently of the pump value, i.e., independently of ε. The terms $\mathbf{u}_{10}$ and $\mathbf{u}_{2i}$ are produced by the nonlinear interaction of the amplitudes of the two marginally stable eigenvectors.

The amplitude equations describe the nonlinear dynamics close to the second threshold, i.e., when the unstable eigenvalue is positive, but small. Under this hypothesis, the dynamics of the terms $\mathbf{u}_{ij}$, of φ_{00} and L_{11} is slow in both space and time,

$$\mathbf{u}_{ij}(\varepsilon z,\varepsilon t,\varepsilon^2z^2,\varepsilon^2t^2,\ldots),$$

$$\varphi_{00}(\varepsilon z,\varepsilon t,\varepsilon^2z^2,\varepsilon^2t^2,\ldots),$$

$$L_{11}(\varepsilon z,\varepsilon t,\varepsilon^2z^2,\varepsilon^2t^2,\ldots).$$

We introduce a control parameter μ defined as

$$\mu=\varepsilon\mu_1+\varepsilon^2\mu_2+\cdots,$$

and slow space and time variables,

$$T_0=t,\quad T_1=\varepsilon t,\quad T_2=\varepsilon^2t^2,\ldots,$$

$$Z_0=z,\quad Z_1=\varepsilon z,\quad Z_2=\varepsilon^2z^2,\ldots,$$

so that the linearized operator defined in Eq. (3) is expanded in

$$\begin{pmatrix} -\kappa+\partial_z & \kappa & 0 & 0 & 0 \\ 1 & -1 & f_0 & 0 & 0 \\ -\gamma_\parallel f_0 & -\gamma_\parallel f_0 & -\gamma_\parallel & 0 & 0 \\ 0 & 0 & 0 & -(1+\kappa) & -\partial_z \\ 0 & 0 & 0 & \kappa & \partial_z \end{pmatrix} = \begin{pmatrix} -\kappa+\partial_{Z_0} & \kappa & 0 & 0 & 0 \\ 1 & -1 & \tilde{f} & 0 & 0 \\ -\gamma_\parallel \tilde{f} & -\gamma_\parallel \tilde{f} & -\gamma_\parallel & 0 & 0 \\ 0 & 0 & 0 & -(1+\kappa) & -\partial_{Z_0} \\ 0 & 0 & 0 & \kappa & \partial_{Z_0} \end{pmatrix}$$

$$+\varepsilon \begin{pmatrix} \partial_{Z_1} & 0 & 0 & 0 & 0 \\ 0 & 0 & \mu_1 & 0 & 0 \\ -\gamma_\parallel \mu_1 & \gamma_\parallel \mu_1 & 0 & 0 & 0 \\ 0 & 0 & 0 & 0 & -\partial_{Z_1} \\ 0 & 0 & 0 & 0 & \partial_{Z_1} \end{pmatrix} + O(\varepsilon^2)$$

$$= \mathcal{L}_0(q) + \varepsilon \mathcal{L}_1 + O(\varepsilon^2),$$

where the symbol $\mathcal{L}_0(q)$ highlights the fact that only the order zero term of the expansion depends on the wave vector of the modulation.

The laser equations, (2), can be written as

$$(\partial_{T_0} + \varepsilon \partial_{T_1})(\mathbf{u}_0 + \varepsilon \mathbf{u}_1) = [\mathcal{L}_0(q) + \varepsilon \mathcal{L}_1](\mathbf{u}_0 + \varepsilon \mathbf{u}_1) + \mathcal{N}(\mathbf{u}_0, \mathbf{u}_1) + O(\varepsilon^2),$$

where $\mathcal{N}(\mathbf{u})$ are the nonlinear terms. The amplitude equations are obtained by expanding this equation in powers of ε and by imposing that at each order the equation

$$\mathcal{L}_0(q)\mathbf{u}_n = \mathbf{S}_n, \tag{12}$$

where $\mathbf{S}_n$ is a source term function of the slow derivatives and of the amplitudes of order lower than n, is solvable. The operator $\mathcal{L}_0(q)$ is noninvertible for $q=0$ and $q=\tilde{q}$. Therefore this equation is solvable only if

$$\mathbf{S}_n \cdot \mathbf{v}_i = 0, \tag{13}$$

where $\mathbf{v}_i$, $i=0,1$, are the kernels of the adjoint of the matrices $\mathcal{L}_0(0)$ and $\mathcal{L}_0(\tilde{q})$, respectively.

Equation (13) is the amplitude equation up to order n. The algebra involved in obtaining them is rather heavy and we have written a Maple procedure to obtain them up to third order in ε. However, their form can be derived by using symmetry arguments [11]. The purpose of the Maple procedure is, then, to provide the numerical values of the various coefficients.

Let us start by the phase equation, the equation for $\hat{\varphi} = \Sigma_n \varepsilon^n \varphi_{n0}$ (we have shown in the previous section that $\mathbf{w}_1$ is the global phase of the field). We can make the following observations: (1) The equation must be real, since $\hat{\varphi}$ is a real variable. (2) The value of $\hat{\varphi}$ itself does not play any role in the dynamics. The actual value of the phase is irrelevant; what matters are the changes of the phase across the cavity, i.e., $\partial_z \hat{\varphi}$. (3) The phase is marginally stable independently of the value of the pump. Therefore the equation does not contain μ. (4) The nonlinear terms in Eq. (2) do not depend on $\partial_z \varphi$: as a consequence the amplitude equation does not contain a term in $(\partial_z \varphi)^2$. (5) Finally, if $\hat{L} \equiv \Sigma_n \varepsilon^n L_{n1}$ is the amplitude of the unstable mode at wave vector $\tilde{q}$, the only functions of $\hat{L} e^{i\tilde{q}z}$ that can appear in the phase equation must have zero wave vector; i.e., they must be of the form $f(|\hat{L}|^2)$. Therefore a normal form for the phase equation up to third order in ε is

$$\partial_t \hat{\varphi} = \alpha_1 \partial_z \hat{\varphi} + \alpha_2 \partial_{zz} \hat{\varphi} + \alpha_3 |\hat{L}|^2 \partial_z \hat{\varphi}, \tag{14}$$

where α_i, $i=1,3$ are real constants. Moreover it is possible to show [10,12,13] that the coefficients of the linear terms of the amplitude equations are related to the derivatives of the marginally stable eigenvalue, $\lambda(q,\mu)$. In the case of Eq. (14) we have

$$\alpha_1 = -i\partial_q \lambda(0,0), \quad \alpha_2 = -\partial_{qq} \lambda(0,0). \tag{15}$$

Now, for the second equation: (1) The equation for $\hat{L}$ can be complex, $\hat{L}$ itself being a complex variable. (2) The mode is stable for $\mu<0$, unstable for $\mu>0$. Therefore, the equation contains a linear term of the form $(\delta_1 + i\delta_2)\mu\hat{L}$. (3) All the terms that appear in the equation have wave vector $q=\tilde{q}$. Therefore, they must be of the form $f(\partial_z \hat{\varphi}, |\hat{L}|^2)\hat{L}$. (4) Finally, there are no terms in $\partial_z \hat{\varphi} \hat{L}$, since the nonlinear terms in the laser equations, (2), are independent of $\partial_z \hat{\varphi}$. Therefore, the amplitude equation for $\hat{L}$ has the form

$$\partial_t \hat{L} = (\delta_1 + i\delta_2)\mu\hat{L} + \vartheta \partial_z \hat{L} + (\eta_1 + i\eta_2)\partial_{zz}\hat{L} + (\varrho_1 + i\varrho_2) \times (\partial_z \hat{\varphi})^2 \hat{L} + (\sigma_1 + i\sigma_2)|\hat{L}|^2 \hat{L}, \tag{16}$$

where all the terms δ_i, ϑ, η_i, ζ_i, and σ_i are real. The coefficients of the linear terms are related to the derivatives of the marginally stable eigenvalue at $q=\tilde{q}$ by

$$\begin{aligned} (\delta_1 + i\delta_2) &= \partial_\mu \lambda(\tilde{q},0), \\ \vartheta &= -i\partial_q \lambda(\tilde{q},0), \\ (\eta_1 + i\eta_2) &= -\partial_{qq} \lambda(\tilde{q},0). \end{aligned} \tag{17}$$

These relations together with Eqs. (15) are used by the Maple procedure to find the values of the linear coefficients. The values of the nonlinear ones are obtained by solving Eqs. (12) and (13) up to third order in ε.

By scaling space, time and the two variables $\hat{\varphi}$ and $\hat{L}$, and by referring to a suitably rotating and moving reference frame, it is possible to rewrite Eqs. (14) and (16) in a more compact form,

$$\partial_\tau L = \mu L + (1+ic_1)\partial_{\zeta\zeta} L + (1+ic_2)|L|^2 L - (1+ic_3)(\partial_\zeta \varphi)^2 L, \tag{18}$$

$$\partial_\tau \varphi = c_4 \partial_\zeta \varphi + c_5 \partial_{\zeta\zeta} \varphi + c_6 |L|^2 \partial_\zeta \varphi, \tag{19}$$

where

$$\tau = \delta_1 t - z\,\frac{\delta_1}{\vartheta}, \quad \zeta = z\sqrt{\frac{\delta_1}{\eta_1}}, \quad \varphi = \sqrt{-\frac{\varrho_1}{\delta_1}}\,\hat{\vartheta},$$

$$L = \sqrt{\frac{\sigma_1}{\delta_1}}\, e^{i\delta_2 t}\hat{L}, \quad c_1 = \frac{\eta_2}{\eta_1},$$

$$c_2 = \frac{\sigma_2}{\sigma_1}, \quad c_3 = -\frac{\varrho_2}{\varrho_1}, \quad c_4 = \frac{\alpha_1 - \vartheta}{\delta_1},$$

$$c_5 = \frac{\alpha_2}{\eta_1}, \quad c_6 = \frac{\alpha_3}{\sigma_1}.$$

It is immediately recognized that Eq. (18) is a complex Ginzburg-Landau equation (CGL) coupled with a further equation for the global phase. In the next section we discuss the values of the various coefficients, the form of the equations (18) and (19) and we compare their solutions with those of the Maxwell-Bloch equations, Eqs. (1) and (2).

IV. AMPLITUDE EQUATIONS

The coefficients of the amplitude equations are functions of two independent parameters only, the rescaled field- and population-decay rates, κ and $\gamma_\parallel$, respectively. We have determined all the coefficients by means of the Maple procedure for several choices of the two parameters. The numerical values for the Ginzburg-Landau equation are reported in Fig. 2, while those of the phase equation are plotted in Fig. 3. It turns out that the former set of coefficients is independent of κ. This result can be confirmed analytically in the case of the coefficient c_1. From its definition and from Eq. (17), we can write

$$c_1 = \frac{\mathrm{Im}[\partial_{qq}\lambda(\tilde{q},0)]}{\mathrm{Re}[\partial_{qq}\lambda(\tilde{q},0)]}. \tag{20}$$

We know that the marginally stable eigenvalue is, at threshold, purely imaginary and, from Sec. II, that its imaginary part is given by Eq. (9). Moreover, always from Sec. II, we know that $\partial_q \tilde{\nu}$ is a real number: therefore it is equal to the ratio between the real parts of the numerator and of the denominator in Eq. (7). Again, by taking advantage of Eq. (9), we obtain

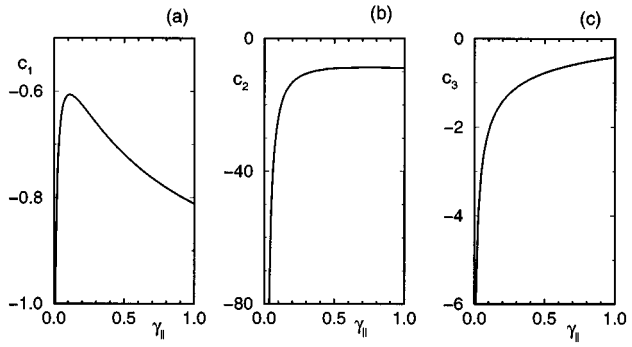

FIG. 2. The three coefficients of the complex Ginzburg-Landau equation (18) vs the only relevant parameter, $\gamma_\parallel$.

$$\partial_q \tilde{\nu} = \frac{2\tilde{\nu}^2(1+\gamma_\parallel)}{2\tilde{\nu}^2(1+\gamma_\parallel) + \kappa\gamma_\parallel(7\tilde{f}^2 - \gamma_\parallel)}, \tag{21}$$

which contains a nontrivial dependence on the parameter κ. Notice that this is the coefficient of $\partial_z L$.

From Eq. (4), and recalling the expression for $\partial_q \nu$, Eq. (21), one obtains

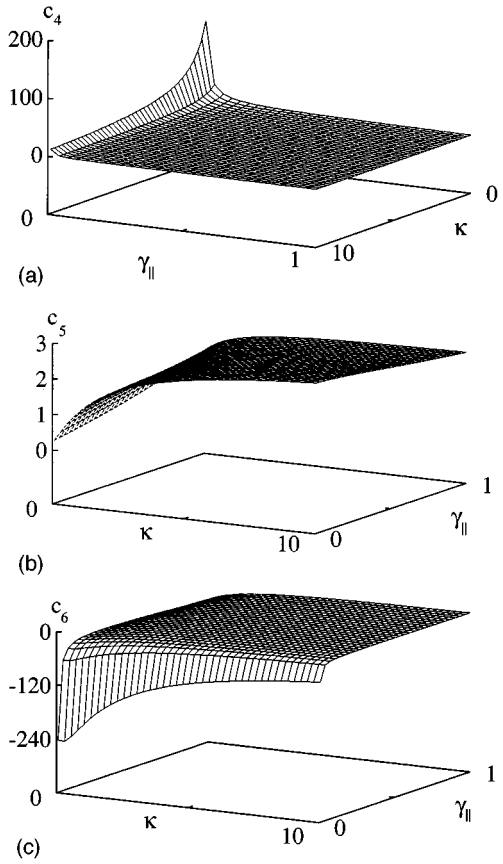

FIG. 3. Surface plots of the three coefficients of the phase equation (19) vs $\gamma_\parallel$ and κ.

$$\partial_{qq}\lambda = 2(\partial_q \tilde{\nu})^2 \frac{3\tilde{\nu}\partial_q\tilde{\nu} - q\partial_q\tilde{\nu} - 2\tilde{\nu} - i(1+\gamma_\parallel+\kappa)\partial_q\tilde{\nu} + i(1+\gamma_\parallel)}{\tilde{\nu}(1+\gamma_\parallel) + i\tilde{\nu}^2 - i(1+\tilde{f}^2)\gamma_\parallel}. \tag{22}$$

Substituting back in Eq. (20) and using Eqs. (9) we find

$$c_1 = \tilde{\nu}\frac{\tilde{f}^2(8-8\gamma_\parallel^2-10\gamma_\parallel+13\gamma_\parallel\tilde{f}^2)+3\gamma_\parallel^2(\gamma_\parallel+2)}{\gamma_\parallel(1+\gamma_\parallel)(-35\tilde{f}^4+18\tilde{f}^2\gamma_\parallel-3\gamma_\parallel^2-8\tilde{f}^2)}, \tag{23}$$

which is independent of κ. Physical considerations on the damping processes reveal that the decay rate of the polarization must be larger than or equal to the decay rate of the population. Accordingly, $\gamma_\parallel$ is bounded to be smaller than 1. For $\gamma_\parallel \to 0$, c_1 diverges to $-\infty$ as $-1/\sqrt{48\gamma_\parallel}$. The overall behavior is reported in Fig. 2(a). A similar proof for the independence of κ other two coefficients, though in principle feasible, would involve so much algebra as to be in the end very obscure. In the absence of any short-cut we just rely on the numerical evidence.

The first general observation about the amplitude equations concerns the sign of the coefficients. The cubic term turns out to have always a positive real part, thus meaning that it has always a destabilizing effect. In other words, we are in the presence of a subcritical Hopf bifurcation, i.e., for pump values smaller than $\tilde{\chi}$, two oscillating solutions coexist together with all stable plane waves. Accordingly, at least in principle, it is possible to observe a nontrivial dynamical behavior below the second laser threshold. Whether this implies the existence of a stable chaotic evolution is an open question that we leave to future investigations. Above threshold, in the absence of any spatial variations of the fields, the positive cubic term indicates that one should include at least the fifth-order contribution to confine the evolution within a finite region of the phase space. Nevertheless, Schöpf and Kramer [5] have shown that if the system is sufficiently dispersive or, more precisely, if $c_2 < 4c_1$, the amplitude of the field L remains bounded. A direct check from the data reported in Fig. 2 reveals that the inequality is always satisfied; indicating that the dynamics of the CGL alone remains confined.

The second comment on the CGL equation refers to its coupling to the phase equation through the last term proportional to L. The real part of its coefficient is always negative, implying that it tends to stabilize the homogeneous solution with $L=0$. A partial explanation of this effect is offered by the analysis of the simple case when $\partial_\zeta\varphi \equiv Q$ is independent of z. A solution with a constant value $Q \neq 0$ of the derivative of its phase is nothing but a nonresonant cavity mode with wave number $k=Q$. A direct linear stability analysis of such modes reveals that they are less unstable than the resonant one, as they bifurcate at larger values of the pump parameter (see Fig. 1).

Thus, the condition $\mu = Q^2$ is nothing but a quadratic approximation of the threshold line of the nonresonant modes and, accordingly, we see that the amplitude equation model accounts also for their evolution.

It is instructive to write the phase equation in terms of the variable Q,

$$\partial_\tau Q = \partial_\zeta(c_4 + c_6|L|^2)Q + c_5\partial_{\zeta\zeta}Q. \tag{24}$$

This is a Fokker-Planck-type equation with Q playing the role of the ''probability distribution,'' although there is no need for it to be positive definite. The configuration $|L|=0$ and $Q=$const is a solution of the equation, as it should, since it is a generic cavity mode. The term $c_4 + c_6|L|^2$ is analogous to a force field and it tends to make the phase drift. In the absence of amplitude fluctuations ($L=0$) it reduces to the standard phase velocity of the cavity modes.

The Fokker-Planck equation conserves the overall probability, a feature that in the laser context becomes the conservation of the average wave number $\langle Q \rangle$, i.e., of the winding number of the global phase. The evolution of resonant solutions can be understood by recalling the spectral properties of the Fokker-Planck operator, which admits only negative eigenvalues except for a single zero component (expressing the probability conservation). In fact, in the resonant case, $\langle Q \rangle = 0$, so that no component of the initial phase configuration lies along the marginally stable direction and the asymptotic solution is necessarily $Q=0$, i.e., the phase tends spontaneously to homogenize. Accordingly, the asymptotic dynamical features are determined only by the Ginzburg-Landau equation. Nevertheless, the corrections to the drift term in the phase equation have a sound physical interpretation. In fact, the term c_4 is nothing but the phase velocity of the single mode (in the rescaled units) that we know to be independent of the wave number k. When the dynamics is switched on, the nonzero average value of $|L|$ induces a correction that can be interpreted as a shift in the group velocity. In fact, the time derivative of φ is a variation $\delta\omega$ in the global frequency, while the spatial derivative is nothing but a variation δk. Thus, we can conclude that the nonlinear dynamics induces a decrease in the group velocity (c_6 turns out to be always negative).

In the nonresonant case, the parameter μ cannot be scaled out any longer. In particular, for $\mu \ll 1$, the drift present in the phase equation is of order 1, while the dynamics of the amplitude L is very slow. Accordingly, the phase dependency in the Ginzburg-Landau equation can be safely averaged over the spatial variable. Since $\langle Q \rangle \equiv \langle \partial_\zeta\varphi \rangle$ is a constant of motion (see the above considerations), the role of the phase is simply to renormalize the control parameter μ to a smaller effective value. Accordingly, the L evolution is still described by a Ginzburg-Landau equation, while $|L|^2$ can be seen as an external chaotic forcing acting on the global phase. This observation suggests introducing a further representation of the phase dynamics by removing the average spatial drift from the global phase, $\psi \equiv \varphi - \langle Q \rangle \zeta$. The variable ψ satisfies the equation

$$\partial_\tau \psi = (c_4 + c_6|L|^2)\partial_\zeta \psi + c_5 \partial_{\zeta\zeta}\psi + (c_4 + c_6|L|^2)\langle Q \rangle. \tag{25}$$

The first term in the right-hand side can be effectively removed by choosing a suitable moving reference frame. In such a case, one is left with a model which is very reminiscent of the Edwards-Wilkinson equation for the interfacial profile height h [14],

$$\partial_\tau h = D\partial_{\zeta\zeta} h + \xi, \tag{26}$$

where ξ is a white noise term with average $\langle \xi \rangle = v$. In fact, the main difference between the above model and Eq. (25) is that the stochastic forcing is substituted by a chaotic fluctuating term resulting from the integration of a CGL. However, we believe that this is not extremely important as long as the evolution of the CGL equation is chaotic with no long-range space-time correlations.

V. NUMERICAL ANALYSIS

To test the correctness of the amplitude equations in the vicinity of the second laser threshold, we have numerically integrated both the original Maxwell-Bloch model and the amplitude equations for the particular choice of parameter values $\gamma_\parallel = \kappa = 1$. In this case, $\tilde{\chi} = 8 + 4\sqrt{3} = 14.9288$, while $c_1 = 0.81161$ and $c_2 = -8.88366$. We have used two different algorithms to integrate both sets of equations: a split step and a pseudo-spectral method, both with periodic boundary conditions. In both cases the space derivatives have been evaluated using a fast Fourier transform routine. A Runge-Kutta algorithm has been used to integrate the nonlinear part of the equations in the split-step program. A variable step variable order Adams algorithm (Nag routine d02cbf) has been used in the pseudo-spectral program. Both codes have produced comparable results. Moreover we have tested the programs by checking that the numerical stability threshold characteristics of the traveling-wave solution coincide with those obtained in Sec. II.

Two typical patterns, one of $|L|$ and one of the electric field amplitude f in the resonant case, are reported in Fig. 4 using two gray-scale images. Space runs from left to right, while time flows downwards. In Fig. 4(a) we see that around the ''defects,'' where two propagating filaments (white stripes) coalesce, L exhibits a sharp peak. The approximately periodic spatial structure reveals the existence of a further spatial scale besides that corresponding to the critical wave number $\tilde{q}$ of the unstable perturbations, obviously absent in this representation, but clearly visible in Fig. 4(b) (the high-frequency ripples). Moreover, we can see from these images how this type of behavior is comparable to the ''dispersive chaos'' phenomenology analyzed in Ref. [6]: peaks of light move in an irregular manner along the cavity never settling down.

A quantitative comparison with the Maxwell-Bloch equations has been done by computing the average square amplitude of the field fluctuations

$$\Delta f = \overline{\langle \delta f^2 \rangle}, \tag{27}$$

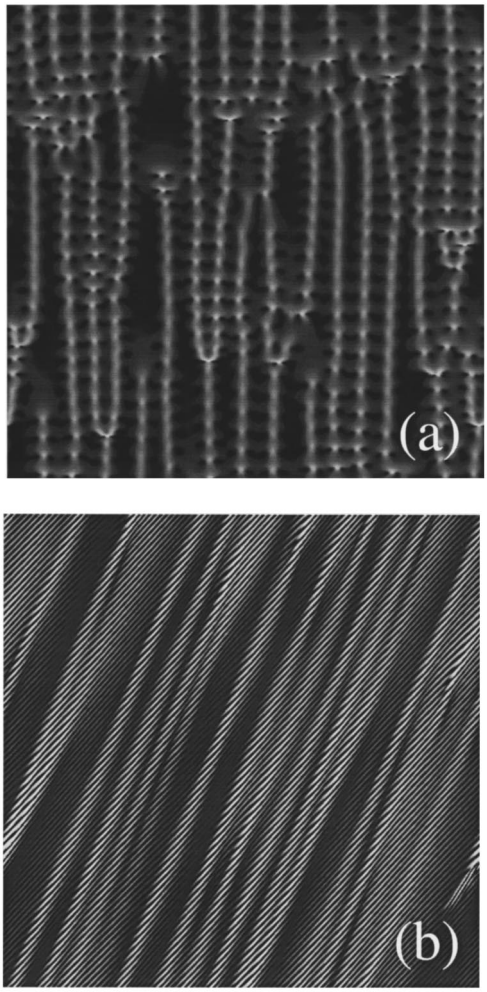

FIG. 4. Gray scale images of the modulus of the field L (a) and of the electric field amplitude f (b) obtained by integrating Eqs. (18) and (1), respectively. The horizontal axis represents the position of the field along the cavity, while time flows downward. The parameters of both simulations correspond to $\kappa = \gamma_\parallel = 1$. Equation (18) has been integrated with $\mu = 1$, for 50 time units on a 512-point grid of total length 50. Equation (1) has been integrated with $\chi = 16$, for 100 time units on a 512-point grid, corresponding to a cavity length 125.

where the overline denotes temporal average. By recalling the scaling transformations adopted to arrive at expression (18), one can also write

$$\Delta f = \frac{1}{2}\left|\frac{\delta_1}{\sigma_1}\right| |w_{21}|^2 \Delta L = 2.452 \Delta L, \tag{28}$$

where ΔL is defined in an equivalent manner to Δf and w_{21} is the first component of $\mathbf{w}_2$. Numerical simulations done at $\mu = 1$ give $\Delta L = 2.12 \pm 0.02$. As μ can be scaled out in the Ginzburg-Landau model, this information suffices to determine the dependence of ΔL on the control parameter. The results of the numerical comparison, reported in Fig. 5, reveal an excellent agreement. The main source of limitations to the applicability of the CGL equation comes from the spikes arising when two nearby filaments coalesce. In fact, it is precisely when $|L|$ is large enough that the perturbative approach may fail. Therefore, we have determined numeri-

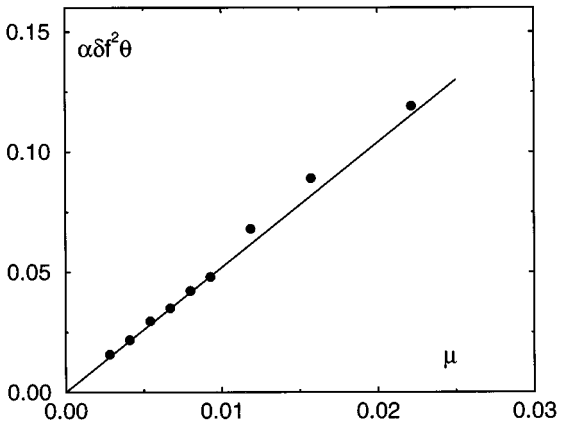

FIG. 5. Average square amplitude of field fluctuations for different values of μ (full circles) compared with the expected value from the CGL equation. All simulations refer to the case $\kappa=\gamma_{\parallel}=1$.

cally the probability density $P(|L|)$ for the same parameter values as above in order to test whether it is bounded from above. The properly rescaled histogram is reported in Fig. 6 where it is seen a clear power-law decay at large intensity values. However, the most important feature is the lack of any evidence of an upper bound to $|L|$. If a spike in $|L|(t)$ has no qualitative consequence on the dynamics, then we may hope that the failure of the amplitude equation is very marginal being observable in a few sporadic events. However, we must notice that when $|L|$ becomes so large as to be comparable with the intensity of the single laser mode, then a defect may occur leading, in turn, to a change of the winding number. In order to test this hypothesis, we have executed a series of long simulations of the Maxwell-Bloch model somehow above threshold (i.e., for $\chi=16$), in which case it is possible to perform a thorough investigation of nonresonant dynamics too.

More precisely, starting from an initial condition with wave number $k(t=0)=k_0$ we have let it evolve for 2000 time units, monitoring $k(t)$. We have then repeated the simulation for 100 different initial conditions [15], to determine the ensemble average $\langle k\rangle$, which is reported in Fig. 7 for four different choices of the wave number (namely $k_0=0$, 0.05, 0.15, and 0.3). In all cases, several small spikes are observed, which represent the signature of temporary jumps of $k(t)$

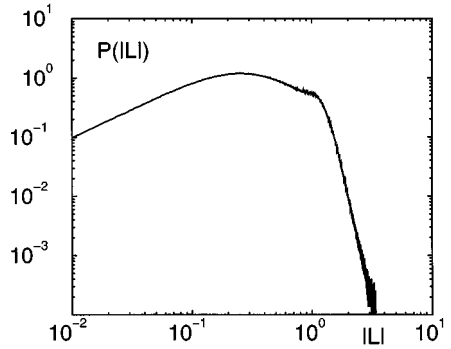

FIG. 6. Probability density $P(|L|)$ of the amplitude $|L|$ as determined from the CGL equation for the same parameter values as in Fig. 5.

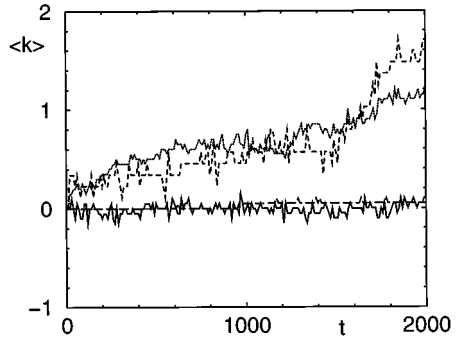

FIG. 7. Average wave vector (winding number) $\langle k\rangle$ vs time for four ensembles of 100 realizations starting with $k(0)=0$ (solid line), 0.05 (dotted), 0.15 (dashed), and 0.3 (long-dashed), respectively.

with no implication on the asymptotic dynamics. The average winding number remains practically constant and equal to the initial value in the evolution of both the perfectly resonant and of the most off-resonant mode. In the former case, this behavior can be explained by symmetry considerations: positive variations of $k(t)$ are equally likely as negative ones. In the latter case, instead, it suffices to notice that a configuration with $k_0=0.3$ corresponds to a point slightly below the marginal stability line L_2 in Fig. 1, so that the extremely rare jumps are to be attributed to the much weaker chaotic evolution. For the two intermediate values of k_0, a clear drift towards nearly stable modes is observed. This implies that ''permanent'' changes of winding number occur too. These phenomena have been described by Ikeda *et al.* in Ref. [4], where the authors introduced the concept of *chaotic itineracy* as a sequence of random jumps among the remnants of former attractors.

Accordingly, the evolution of the wave number is vaguely reminiscent of that of a particle in a symmetric bistable potential, the unstable state corresponding to the resonant mode while the stable states to the marginally stable laser modes. Whether this picture can be taken as a serious starting point for constructing a meaningful model of the laser dynamics is a completely open question. For instance, some preliminary simulations suggest that the permanent changes of winding number, which make $k(t)$ diffuse away from the resonant condition, are more rarefied when the cavity length is increased. However, it is too early to conclude that this phenomenon becomes negligible in the thermodynamic limit (infinite cavity length).

Notice that the above is an important question from an experimental point of view, since a vanishing diffusion of the winding number implies that the chaotic evolution described by the single CGL is a phenomenon observable over all time scales and hence, presumably accessible to experimental investigation. Conversely, a non-negligible role of the defects would imply a nonzero diffusion and, thereby, drift of the wave number towards marginally stable states, thus making the dynamics of the amplitude equation relevant only for a transient time.

VI. CONCLUSIONS AND OPEN PROBLEMS

The weakly nonlinear analysis discussed in this paper shows that the dynamics of the laser just above the second

threshold is approximately described by a CGL equation coupled to a Fokker-Planck equation for the spatial derivative of the global phase. Such a model allows us to predict and describe several features of the numerically observed chaotic evolution. In particular, the highly dispersive CGL accounts for the dynamics displayed by the linearly unstable mode. Moreover, the evolution of the global phase can be connected to that of the unstable modes and their interaction modifies the dispersion properties of the active medium.

Furthermore our results open a Pandora's box, stimulating further investigations along several directions. First of all, one should recall that the amplitude equations are, by construction, correct over a finite range of time scales; thus, it would be desirable to understand to what extent they apply to the asymptotic dynamics in the thermodynamic limit. In the previous section we have discussed one possible source of limitations: the occurrence of sporadic strong spikes whereby a defect can originate. However, one should mention a further limitation associated with the phase dynamics. Indeed, the analogy with Edwards-Wilkinson dynamics uncovered in Sec. IV leads immediately to conjecture that nonlinear (higher-order) terms should exist, which make the correspondence with the Kardar-Parisi-Zhang (KPZ) equation [16] even more appropriate. For those readers who are not familiar with the latter equation, it is worth recalling that it arises by adding a nonlinear term proportional to $(\partial_\xi h)^2$ to the left-hand side of Eq. (26). Such a term provides the leading correction to the linear behavior, changing the asymptotic (in time) growth rate of interfacial (phase in our case) fluctuations. A rapid inspection of the procedure to derive our amplitude equation suggests that the above type of nonlinear corrections should indeed arise at higher orders. We leave to a future analysis the investigation of this point and, in particular, of the scaling behavior of phase fluctuations. We should, in fact, recall that there cannot be an exact equivalence between the field phase evolution and that of a stochastic model such as KPZ equation. The noisy term in the phase equation is, in fact, the result of an intrinsic chaotic evolution rather than being the result of an interaction with an external random environment.

A further aspect that deserves a more detailed investigation is the occurrence of defects. In particular, it should be understood whether defects arise just above the second threshold or whether there is a further transition point (as somehow conjectured in [4]). In this analysis, one should keep in mind a possible dependence of the scenario on the parameter values that in the previous section of this paper have been kept fixed to a specific choice.

Another question that deserves a further analysis is the observed drift of the average wave number $\langle k \rangle(t)$ towards stable modes. Is there a critical frequency above which such a phenomenon appears? This is connected with the possibility of the amplitude equations to provide a quantitative description of the dynamics over all time scales.

Finally, we want to recall that the reverse character of the Hopf bifurcation implies that at least periodic solutions other than single modes exist below the second laser threshold. Whether this phenomenon implies the existence of nontrivial stable behavior even below threshold is another point deserving further investigations.

ACKNOWLEDGMENTS

G.D. was partially supported by a Royal Society and a European Union Human Capital and Mobility grant.

[1] H. Risken and K. Nummedal, J. Appl. Phys. **39**, 4662 (1968).
[2] R. Graham and H. Haken, Z. Phys. **213**, 420 (1968).
[3] L. A. Lugiato, G. L. Oppo, J. R. Tredicce, L. M. Narducci, and M. A. Pernigo, J. Opt. Soc. Am. B **7**, 1019 (1990).
[4] K. Ikeda, K. Otsuka, and K. Matsumoto, Prog. Theor. Phys. Suppl. **99**, 295 (1989).
[5] W. Schöpf and L. Kramer, Phys. Rev. Lett. **66**, 2316 (1991).
[6] J. Glazier, P. Kolodner, and H. Williams, J. Stat. Phys. **64**, 945 (1991).
[7] L. Lugiato, L. Narducci, E. Eschenazi, D. Bandy, and N. Abraham, Phys. Rev. A **32**, 1563 (1985).
[8] L. Narducci, J. Tredicce, L. Lugiato, N. Abraham, and D. Bandy, Phys. Rev. A **33**, 1842 (1986).
[9] P. Gerber and M. Büttiker, Z. Phys. B **33**, 219 (1979).
[10] P. Manneville, *Dissipative Structures and Weak Turbulence* (Academic Press, Boston, 1990).
[11] P. Coullet, S. Fauve, and E. Tirapegui, J. Phys. (Paris) Lett. **46**, L787 (1985).
[12] J. Moloney and A. Newell, *Nonlinear Optics* (Addison-Wesley, Redwood City, CA, 1991).
[13] M. C. Cross and P. C. Hohenberg, Rev. Mod. Phys. **65**, 851 (1993).
[14] S. F. Edwards and D. R. Wilkinson, Proc. R. Soc. London Ser. A **381**, 17 (1982).
[15] Every new initial condition has been obtained from the last configuration of the previous realization, uniformly changing both field and polarization phases in such a way as to set back the wave number equal to the assigned value k_0. This procedure allows us to get rid of the long transients needed to reach an asymptotic state, starting from random configurations.
[16] M. Kardar, G. Parisi, and Y.-C. Zhang, Phys. Rev. Lett. **56**, 889 (1986).